Optimal multivalent targeting of membranes with many distinct receptors

Tine Curk[a,b], Jure Dobnikar[a,b,c,1], and Daan Frenkel[b,1]

[a]CAS Key Laboratory of Soft Matter Physics, Beijing National Laboratory for Condensed Matter Physics, Institute of Physics, Chinese Academy of Sciences, Beijing 100190, China; [b]Department of Chemistry, University of Cambridge, CB2 1EW Cambridge, United Kingdom; and [c]School of Physical Sciences, University of Chinese Academy of Sciences, Beijing 100049, China

This contribution is part of the special series of Inaugural Articles by members of the National Academy of Sciences elected in 2016.

Contributed by Daan Frenkel, May 30, 2017 (sent for review March 13, 2017; reviewed by Michael P. Brenner and Ludwik Leibler)

Cells can often be recognized by the concentrations of receptors expressed on their surface. For better (targeted drug treatment) or worse (targeted infection by pathogens), it is clearly important to be able to target cells selectively. A good targeting strategy would result in strong binding to cells with the desired receptor profile and barely binding to other cells. Using a simple model, we formulate optimal design rules for multivalent particles that allow them to distinguish target cells based on their receptor profile. We find the following: (*i*) It is not a good idea to aim for very strong binding between the individual ligands on the guest (delivery vehicle) and the receptors on the host (cell). Rather, one should exploit multivalency: High sensitivity to the receptor density on the host can be achieved by coating the guest with many ligands that bind only weakly to the receptors on the cell surface. (*ii*) The concentration profile of the ligands on the guest should closely match the composition of the cognate membrane receptors on the target surface. And (*iii*) irrespective of all details, the effective strength of the ligand–receptor interaction should be of the order of the thermal energy k_BT, where T is the absolute temperature and k_B is Boltzmann's constant. We present simulations that support the theoretical predictions. We speculate that, using the above design rules, it should be possible to achieve targeted drug delivery with a greatly reduced incidence of side effects.

multivalency | Monte Carlo simulations | drug delivery | endocytosis | statistical mechanics

The fact that most cells can be recognized from the outside is advantageous for the normal functioning of an organism, but it can be a disadvantage when specific cells are being targeted by pathogens. Cells betray their identity (and state of health) by the composition profile of molecules that are exposed on their outer surface. In what follows, we call these molecules "receptors," irrespective of whether they are receptors in the biological sense (they are receptors for the ligands that will be used to recognize them). It would clearly be advantageous if diseased cells could be selectively targeted by a drug-delivery vehicle on the basis of their receptor profile. Here, the crucial word is "selective": We wish to target only those cells that have the correct receptor profile, as binding of drug-delivery vehicles to other cells may lead to undesired side effects.

Targeted drug delivery is based on identifying a specific marker (peptide, sugar) that is unique to the targeted group of cells. Binding to a single marker type can be effective if this molecule is presented in sufficient quantities on the outer surface of the targeted cell. However, in many cases of practical importance (e.g., many types of cancer), the markers that are known are not unique to cancer cells, but just overexpressed. Over the past 20 y many nanoparticle-based targeting methods have been developed. However, thus far, effective tumor drug delivery is hampered by the lack of reliable, unique markers (1, 2).

To recognize the simultaneous presence of a mixture of different receptors on the host surface, we need to use a "guest" particle (e.g., drug-delivery vehicle) that is coated with a mixture of cognate ligands schematically shown in Fig. 1. In its simplest form (the binding of dimeric bispecific antibodies compared with monomeric antibodies), this problem has been studied theoretically (3) and experimentally (4). The in vitro experiments showed that the use of bispecific antibodies led to a higher specificity than can be achieved with their standard, monomeric counterparts. However, antibodies are not very good at distinguishing between surfaces that have different receptor concentrations. Such selectivity can be achieved by exploiting multivalency. A series of recent experimental and theoretical papers have shown that multivalent carriers (nanoparticles or polymers) can distinguish target surfaces (cells) on the basis of their receptor concentration, rather than just on the basis of the presence of a suitable receptor (5–9).

The use of multivalent particles coated with a single type of ligand is very effective, provided that a cognate receptor has been identified that is sufficiently overexpressed in targeted cells. But often the situation is not that clear cut (Fig. 1). In general, it is essential to exploit all of the information that we have about the concentration of various receptors on the cell surface and then design guest particles that target this specific receptor profile. In this paper, we show that the design rules for such multicomponent targeting are surprisingly simple and therefore hopefully useful. Specifically, we show that the individual ligand–receptor binding strength needs to be weak, such that when the guest particle is within interaction range of the surface, each ligand is unbound 30% of the time. To target a specific receptor profile selectively, many weak ligands work better than a few strong ones. We derive our results using a simple analytical theory and

Significance

A key challenge in biomedical research is the ability to specifically target cells and tissues. Targeting typically relies on identifying a suitable marker, e.g., a highly expressed receptor, and choosing a ligand that strongly and specifically binds to the marker. However, this procedure fails when a suitable marker unique to the targeted cells cannot be identified, notably in many forms of cancer. We show that properly designed multivalent targeting of multiple cognate receptor types results in a specificity toward a chosen receptor density profile, thus demonstrating a general route toward targeting cells without particularly dominant markers.

Author contributions: T.C., J.D., and D.F. designed research; T.C. performed research; T.C. analyzed data; and T.C., J.D., and D.F. wrote the paper.

The authors declare no conflict of interest.

Reviewers: M.P.B., Harvard University; and L.L., École Supérieure de Physique et de Chimie Industrielles de la Ville de Paris.

Freely available online through the PNAS open access option.

[1]To whom correspondence may be addressed. Email: df246@cam.ac.uk or jd489@cam.ac.uk.

This article contains supporting information online at www.pnas.org/lookup/suppl/doi:10.1073/pnas.1704226114/-/DCSupplemental.

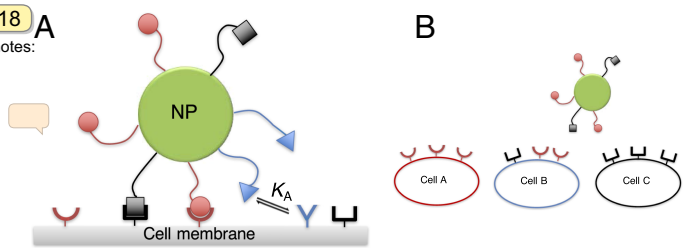

Fig. 1. This schematic figure aims to explain the challenge addressed in this paper. *A* shows a schematic drawing of a multivalent nanoparticle binding to a surface containing several distinct receptors (represented as different concave shapes). *B* shows the challenge: How to target cell B selectively, in the presence of cell types A and C.

validate our approach using coarse-grained simulations. As an example, we present simulation results (Fig. 2) showing that correctly functionalized guest particles are more successful at entering cells with matching receptor compositions than those with suboptimal compositions.

Of course, there is a wide variety of possible host–guest interactions that we could have considered: The receptors could be mobile or immobile, clustered or mixed, etc. In what follows we assume that the host cell is large compared with the guest particle and that the receptors are mobile on its surface. In this case, the chemical potential of the receptors is effectively fixed and, as shown in *SI Appendix*, the theoretical expressions for the binding free energy become surprisingly simple. The other situations that we mention can also be modeled, and the overall conclusions remain the same, except in the limit where so many guest particles bind to the host surface that they deplete the receptor "reservoir." Hence, for the sake of simplicity, we consider just the easiest case. We do not specify the precise nature of the guest particle: It could be a functionalized nanoparticle, polymer, or self-assembled DNA-origami structure. Again, for the present analysis the distinction is immaterial. What is important is that the ligands are flexible and can reach multiple receptors on the surface equally well.

Model

The membrane surface is covered by a population of receptors of different types j with concentrations $\mathbf{c}=\{c_j\}$. Similarly, a multivalent particle is characterized by the ligand composition $\{m_i\}\equiv m\{p_i\}$, where m is the total number of ligands on the guest particle and $\mathbf{p}$ specifies their relative profile; i.e., the relative coverage of the particle with ligands of type i is $p_i=m_i/m$. We are interested in the case where guest nanoparticles interact with a fluctuating number of receptors on the surface. Hence, following the Bell adhesion model (10), the number of receptors in contact with the nanoparticle is not fixed, but their chemical potential is. In contrast, the number of ligands on the nanoparticle that can interact with the surface is fixed. The nanoparticle is attracted to the surface only through ligand–receptor interactions. Apart from that, the particle behaves like a hard sphere (Fig. 1). The ligand–receptor binding is valence limited; i.e., only a single ligand can bind to a receptor and vice versa. The model is an extension of the model of refs. 5 and 7, generalized to include different ligand/receptor types.

To calculate the binding free energy we need to consider all possible bonding combinations between receptors and ligands. To simplify the description, we neglect the interactions between different receptors and we assume that different ligands bind independently (except that no two ligands can bind to the same receptor). The probability that a single ligand i and a single receptor j form a bond depends on the equilibrium constant K_{ij}^A for their association in solution and on the free-energy cost ΔG_i^{cnf}, which is due to the loss of configurational entropy of the ligand upon binding. The configurational entropy term ΔG_i^{cnf} obviously depends on the distance between the receptor and the grafting point of the ligand, which we capture in the simulations. However, it turns out that the distance dependence of ΔG_i^{cnf} is not important in a simple theoretical description: In *SI Appendix* we show that we can treat the configurational term as if it were a constant ($\Delta G_i^{cnf}=\Delta\tilde{G}_i^{cnf}$) for all receptors within a distance h_0 of the ligands and infinite elsewhere. The parameter h_0 represents the ligand–receptor interaction range and is determined by the length of the polymeric linker.

For a ligand within the interaction range of the receptor-decorated surface, the ratio between the probabilities of being in the bound and free (unbound) states is

$$\frac{P_{ij}^{\text{bound}}}{P_i^{\text{free}}}=c_j K_{ij}^A\,\frac{e^{-\beta\Delta\tilde{G}_i^{cnf}}}{h_0}\equiv c_j K_{ij}. \qquad [1]$$

We have defined the effective association constant matrix $\mathbf{K}$, which includes the configurational contribution. Note that the first index i in K_{ij} always refers to a ligand, and the second index j always refers to a receptor. Thus, K_{ii} describes the equilibrium constant for binding between ligand i and its cognate receptor i. Emphatically, it does not mean that ligand i and receptor i are the same species. Similarly, K_{ij} describes the "cross"-binding of ligand i with the receptor cognate to ligand j. K_{ij} is, in general, not the same as K_{ji}, which describes the cross-binding of ligand j with receptor cognate to ligand i. Using the fact that probabilities must add to unity, $P_i^{\text{free}}+\sum_j P_{ij}^{\text{bound}}=1$, we can directly determine the probability that a given ligand is unbound, $P_i^{\text{free}}=(1+\sum_j c_j K_{ij})^{-1}$.

As shown in *SI Appendix*, the fact that the receptors do not interact with each other and are in contact with a reservoir (the remainder of the cell surface) simplifies the expression of the binding free energy between a guest particle and a host

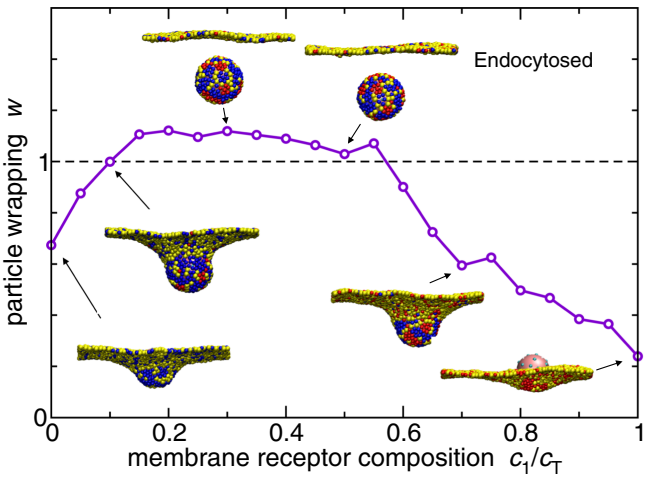

Fig. 2. Simulation results of nanoparticle endocytosis. We consider a system with two ligand types on the particle and two cognate receptor types in the membrane with concentrations c_1 and c_2, respectively. The red and blue beads in the membrane denote receptors of type 1 and type 2, respectively. The yellow beads are inert (no binding to the ligands). The total concentration of receptors is kept fixed at $c_1+c_2=c_T=0.4$, but the composition c_1/c_T is varied. The curve shows the coverage of the particle by the membrane beads (particle wrapping). When the wrapping exceeds 1, the particle is fully covered and has therefore undergone endocytosis. Snapshots show corresponding system configurations. The nanoparticle is covered with 40 randomly distributed immobile ligands with a "ligand" profile $p_1=1-p_2=0.3$. The interaction strength of a ligand patch i is determined as $\epsilon_i=\epsilon^*-\ln(p_i)$, with $\epsilon^*=5k_BT$ for the above results.

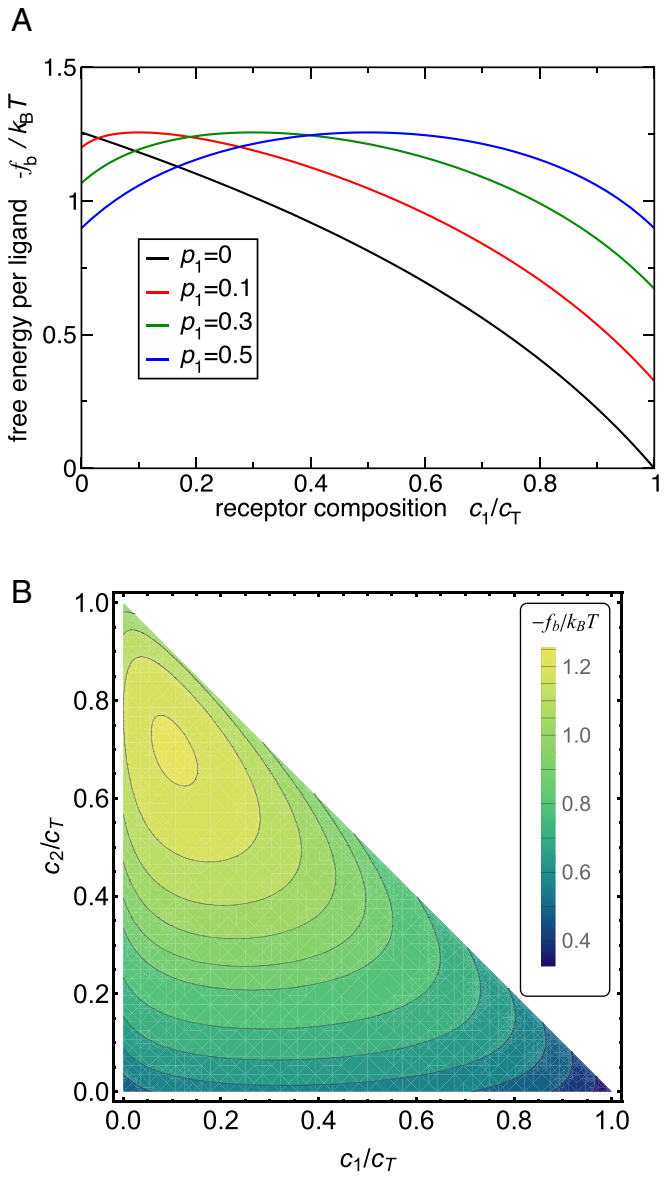

Fig. 3. Optimal targeting using the analytical theory. (*A*) The binding free energy f_b per ligand as a function of the cell receptor composition for two ligand/receptor types. Different curves correspond to different guest profiles $p_1 = 1 - p_2$. (*B*) Targeting with three ligand types. Contour plot shows the binding free energy as a function of the receptor composition c_1 and c_2. The ligand profile is chosen as $\mathbf{p} = [0.1, 0.2, 0.7]$. We have used Eq. **2** to calculate the free energy, assuming a diagonal interaction matrix $\mathbf{K}$ and optimal $\lambda_p = 1.256$.

membrane. Moreover, we assume that different ligands are uncorrelated; hence the binding free energy of the guest particle is simply a sum of individual ligand contributions, $\Delta F_b = m f_b$, with f_b the binding free energy per ligand:

$$f_b = \sum_i p_i \ln P_i^{\text{free}} = -\sum_i p_i \ln\left(1 + \sum_j c_j K_{ij}\right). \quad [2]$$

We note that this expression could be interpreted as (minus) the cross-entropy between the two distributions p_i and P_i^{free}. The total binding free energy for a guest particle near the cell surface is $\Delta F = \Delta F_b + \Delta F_0$, where ΔF_0 is the zero-bond free-energy cost of bringing a guest particle into a position to start forming bonds with the host membrane. For what follows, F_0 is unimportant, because we assume that it is the same irrespective of the receptor composition or the ligand profile, and thus it drops out of the expressions for free-energy difference that determine the selectivity. We note that the host–guest binding free energy is related to the widely used "avidity" constant $K_{av}^A = e^{-\Delta F/k_BT}/\rho_0$, measuring the association between multivalent entities in units of standard molar concentration $\rho_0 = 1$ M.

Furthermore, the same free-energy expression (Eq. **2**) also governs the free-energy change upon a passive particle endocytosis (Fig. 2) where ligands are not flexible, but the membrane itself is. In this case ΔF_0 simply refers to the particle endocytosis free-energy change when there are no receptors present, and ΔF_b again captures bonding with mobile receptors.

Selectivity Optimization

Expression **2** describes how the binding free energy depends on the receptor composition $\mathbf{c}$, particle profile $\mathbf{p}$, and the interaction matrix $\mathbf{K}$.

Our aim is to design a guest particle that binds more strongly to cells with the specified receptor profile $\boldsymbol{c}^*$ than to any other. Among all possible receptor compositions $\mathbf{c}$, the targeted composition $\mathbf{c}^*$ should thus be the one with the minimum binding free energy. This yields the condition

$$\left.\frac{\partial f_b(\mathbf{c}, \mathbf{p}, \mathbf{K})}{\partial \mathbf{c}}\right|_{\mathbf{c}=\mathbf{c}^*} = 0. \quad [3]$$

Note that this equation does not imply that we optimize the receptor composition of the target cell (after all, this composition is given). Rather, we vary the parameters that characterize the guest particle (namely $\mathbf{p}$ and $\mathbf{K}$) to make the guest particle bind more strongly to the target receptor composition than to any other. Because there are several combinations of $\mathbf{p}$ and $\mathbf{K}$ that can satisfy this condition, we need to further select the one that is the most selective, i.e., the one that results in the free-energy minimum with the largest curvature.

Our optimization condition is therefore to maximize the selectivity $\mathcal{S}$, defined as

$$\mathcal{S} = \det\left(\frac{\mathbf{H}(f_b)}{|f_b|}\right)_{\mathbf{c}=\mathbf{c}^*}, \quad [4]$$

subject to the constraint of Eq. **3**. $\mathbf{H}(f_b)$ in Eq. **4** is the (Hessian) matrix of second derivatives of the free energy with respect to composition $\mathbf{c}$. As can be seen from Eq. **4**, the selectivity $\mathcal{S}$ is defined as the relative curvature of the free-energy functional at its minimum.

It is important to define the selectivity as the relative, rather than the absolute, curvature. The absolute value of the free energy can be trivially controlled by changing the number of bonds m, Eq. **2**. Therefore, by optimizing for the relative curvature, we obtain the largest possible curvature at a given absolute value of the free energy ΔF_b. The binding can always be made stronger by increasing the total receptor concentration (5–7, 11); therefore, to make a meaningful comparison, we compare systems with the same total receptor concentration $c_T \equiv \sum_i c_i$ on the membranes.

In general, finding the maximal selectivity by solving for the above conditions is nontrivial and must be performed numerically. However, we can greatly simplify the problem and find a closed-form solution by also requiring that the binding free energy is optimized with respect to the ligand profile $\mathbf{p}$:

$$\left.\frac{\partial f_b(\mathbf{c}, \mathbf{p}, \mathbf{K})}{\partial \mathbf{p}}\right|_{\mathbf{c}=\mathbf{c}^*} = 0. \quad [5]$$

This is in principle not a necessary condition for selective targeting; however, we expect it to be a practically useful condition; we wish to design guests that are robust to small variations in the ligand profile. Robustness is important for practical applications

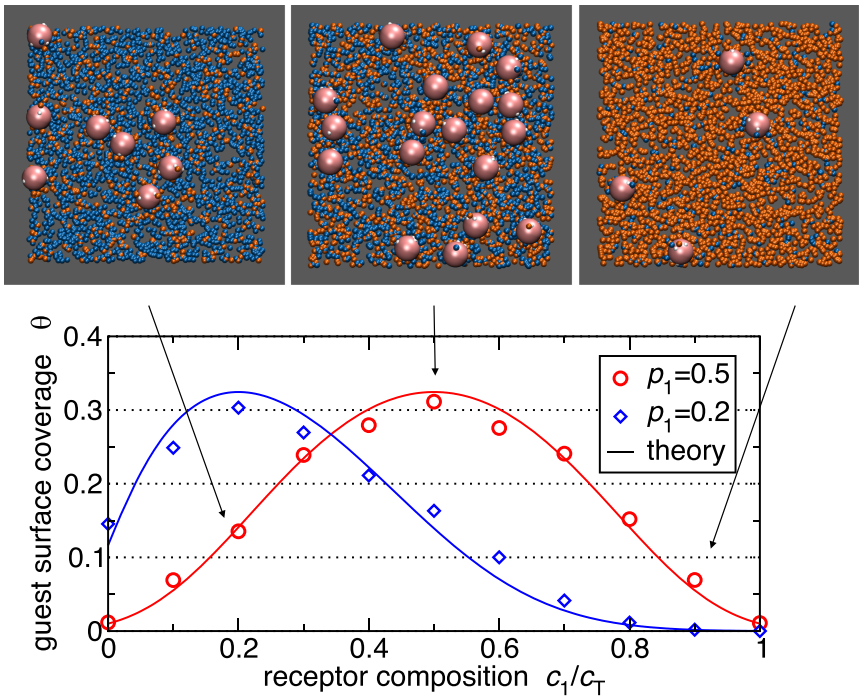

Fig. 4. Grand canonical Monte Carlo simulation results of guest adsorption (symbols) and comparison with analytical theory (solid lines). The simulated surface has two different types of receptors embedded (colored orange and cyan, respectively). The total concentration of receptors is kept fixed at $c_T = 7/R^2$, with R the guest particle radius. Each guest particle has 10 ligands (each represented as a soft blob with radius r_b) with a profile of $p_1 = 0.5$ (red circles) and $p_1 = 0.2$ (blue diamonds) and cognate bond energy $\epsilon = -4.5 k_B T$. The guest chemical potential corresponds to a bulk solution concentration of $\rho = 10^{-6}(2R)^{-3}$. Theoretical adsorption curves (solid lines) are obtained by inserting the free-energy expression Eq. **2** at $\lambda_p = 1.33$ into a standard Langmuir adsorption model, assuming each guest occupies an area of $A = (2R + 2r_b)^2$. The surface coverage θ is the number of adsorbed guests per guest area A. The three snapshots correspond to the plotted data (red circles) at composition $c_1/c_T = 0.2$, 0.5, 0.9 and guest profile $p_1 = 0.5$.

70-72 3 notes: when the guest particle manufacturing-process tolerances must also be considered. The additional constraint results in a simple closed-form solution whereas the optimal selectivity decreases only marginally (*SI Appendix*).

We can determine the optimal ligand profile $\mathbf{p}$ and interaction matrix $\mathbf{K}$ analytically. The procedure that we use is discussed in *SI Appendix*; here we outline only the main results. Our first 73-75 3 notes: result is that all ligands should have the same probability to be unbound,

$$P_i^{\text{free}} = e^{-\lambda_p} = const, \qquad [6]$$

76-79 4 notes: and that each ligand contributes an equal amount, $-\lambda_p k_B T$, to the total binding free energy. Hence, any ligand profile $\mathbf{p}$ will yield the same free energy, $f_b = -\lambda_p k_B T$. In a sense, this result is trivial: It simply states that if all ligands are equally likely to bind, a small change in the ligand profile will not change the overall host–guest binding free energy. This result should not be viewed as a design rule to "target" guest particles by cells (in fact, the rule states that, in the optimal case, the cells cannot distinguish between different particles). Rather, we are interested in the opposite problem, namely the targeting of cells by guest particles. That problem does have a unique, nontrivial solution.

80 iago Rodriguez

81-83 3 notes: Minimizing the free-energy functional Eq. **2** with respect to the particle profile $\mathbf{p}$ and targeted composition $\mathbf{c}^*$ determines the optimal ligand profile $\mathbf{p}^*$. For a symmetric interaction matrix $\mathbf{K}$ (or when off-diagonal terms are small) the ligand profile should match the cognate receptor composition: $\mathbf{p}^* = \mathbf{c}^*/c^T$. Finally, the selectivity $\mathcal{S}$ can be decomposed into a part that depends only on λ_p and a reduced Hessian $\hat{\mathbf{H}}$ that does not,

$$\mathcal{S} = \left[\frac{\left(1 - e^{-\lambda_p}\right)^2}{\lambda_p}\right]^{d-1} \det(\hat{\mathbf{H}}), \qquad [7]$$

where d is the "dimensionality" (the number of distinct receptor types). Optimizing the selectivity, $\frac{\partial \mathcal{S}}{\partial(\lambda_p)} = 0$, we find that the nontrivial solution satisfies $e^{\lambda_p} - 2\lambda_p + 1 = 0$, and hence

$$\lambda_p \approx 1.256\cdots. \qquad [8]$$

Eq. **8** is our most important result. It states that the binding free energy of each ligand to the targeted surface should be $f_b = -\lambda_p k_B T \approx -1.3 k_B T$ irrespective of the details of the system. Equivalently, Eq. **8** states that when the guest particle is adsorbed on the targeted surface, each ligand should be unbound 30% of the time: $P_i^{\text{free}} = e^{-\lambda_p} \approx 0.3$.

Fig. 3 shows the variation of the binding free energy with changing receptor composition obtained from the analytical model. In practice we might wish to distinguish a host surface with 20–80% receptor composition from a surface with inverted 80–20% composition. In Fig. 3 we see that the difference in the corresponding bond strength is about $\Delta f_b \sim 0.5 k_B T$ per ligand. This may not seem to be much, but multivalent guests will hold 10–20 ligands (or more) if we require a total guest binding free energy of the order of $\Delta F_b \sim -10 - 25 k_B T$. The difference thus becomes substantial $\Delta\Delta F_b \sim 5 - 10 k_B T$, corresponding to orders of magnitude difference in adsorption and, therefore, very strong targeting efficacy as shown in Fig. 4.

Furthermore, Fig. 3*B* demonstrates that increasing the number of ligand types increases the selectivity because the optimal binding region becomes a smaller fraction of the total parameter space.

Design Rules

Our analytical calculations suggest the following simple design rules to make multivalent guest particles that target a particular receptor profile:

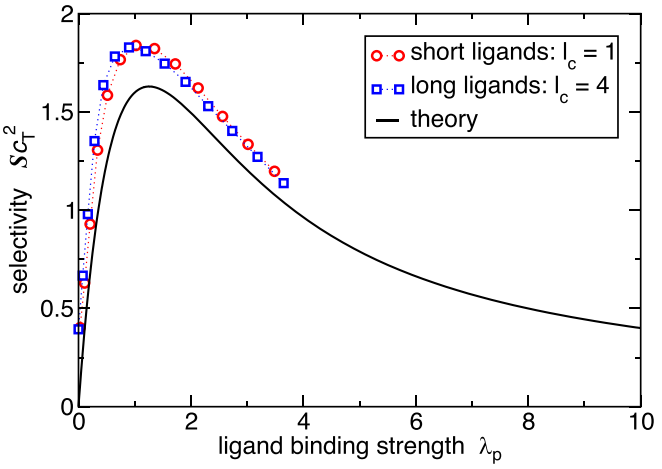

Fig. 5. Selectivity dependence on the mean bond strength λ_p. The theoretical curve is given by Eq. **7**. The simulation results were obtained by calculating the free-energy profile $f_b^{sim}(\mathbf{c}, \mathbf{p}^*, \mathbf{K})$ of a simulated guest particle and obtaining the relative curvature, and hence the selectivity $\mathcal{S}$, from a parabolic fit to the free-energy profile. The mean bond strength from simulations is defined as the free energy per bond at the targeted composition $\lambda_p = -f_b^{sim}(\mathbf{c}^*, \mathbf{p}^*, \mathbf{K})/k_BT$. The simulated guest parameters are chosen according to our analytical design rules, $\mathbf{p}^* = [0.5, 0.5]$.

84-87 4 notes:

- $p_i = c_i/c_T$: Ideally, the profile of the nanoparticle should match the density composition of the targeted cell. As shown in *SI Appendix*, this is not a condition on the average ligand profile. It really means that, ideally, every nanoparticle should have precisely the optimal number of ligands. In fact, if only the averages are fixed and the number of ligands is Poisson distributed, most of the selectivity is lost.

88-89 2 notes:

90-92 3 notes:

- $K_{ii} = \frac{e^{\lambda_p} - 1}{c_i}$: The value of K_{ii} should be inversely proportional to the density c_i. It is useful to avoid cross-binding (i.e., interaction matrix $\mathbf{K}$ should be diagonal). The optimal binding free energy per ligand $\lambda_p \approx 1.3$, which states that ligand binding should be weak, with each ligand independently having the probability of being bound at most 70%.

93-98 6 notes:

99-104 6 notes:

- The greater the number is of distinct ligand–receptor types, the higher the potential selectivity.

- The overall binding free energy ΔF of the particle is proportional to the number of ligands per guest particle (valency m). Valency should be chosen to give a desired absolute value of guest adsorption strength; for Langmuir adsorption the optimal will be close to the chemical potential of the guests in solution $\Delta F \sim \mu$.

105-106 2 notes:

The major assumption underlying the derivation of the design rules is that all pairs of ligands and receptors can in principle form a bond. This assumption is fulfilled when both the ligands and the receptors are mobile, which is often the case in biological systems. However, our results also apply in other situations with some additional restrictions: (*i*) For mobile ligands on the guest but immobile receptors on the membrane, the theory is relevant when the receptor density is large enough. If $A_{cont} \approx R^2$ is the surface area of the membrane in contact with the guest particle, the receptor concentration should be large enough, $c_i > m_i/A_{cont}$, such that all ligands m_i can find their binding partners. (*ii*) In the case of mobile receptors and immobile ligands, the ligand profile p presented to the surface receptors must be independent of the guest particle orientation. This can be achieved when using a long, flexible ligand $h_0 > R$, or when targeting a deformable membrane that can wrap around a particle (Fig. 2), or by carefully uniformly coating the guest particle with ligands such that every "face" presents the same ligand profile. (*iii*) When both ligands and receptors are immobile, both constraints *i* and *ii* apply and in addition each ligand must be able to find a receptor within its interaction range h_0: $c_i > 1/h_0^2$.

Monte Carlo Simulation Results

The above analytical model is highly idealized. However, the coarse-grained simulation results of both particle endocytosis (Fig. 2) and adsorption (Fig. 4) support the predictions of our analytical model. Our simulations clearly show that our design rules, even though derived from a simple model, are nevertheless directly applicable to more complex and realistic systems where ligand interactions, correlations, and membrane elasticity cannot be neglected.

The simulation snapshots of multivalent nanoparticle targeting in Fig. 4 give a pictorial illustration of the effect of optimizing the ligand concentration profile to target a mixed receptor surface. The adsorption isotherm is well captured by the simple analytical model. Furthermore, Fig. 5 shows the selectivity, obtained from the analytical theory (Eq. **4**) and simulations, plotted as a function of the ligand binding strength λ_p. Clearly, the simulation results support the analytical value for the optimal ligand strength $\lambda_p \approx 1.3 k_B T$.

Conclusions

In this paper, we outline simple rules to design ligand-coated particles that can target cell surfaces on the basis of a receptor profile, rather than on the recognition of a single receptor. The receptor profile of a cell surface can be viewed as a "bar code" that is selectively recognized by the ligand profile of the guest particle. Here we have shown that properly designed multivalent targeting of multiple cognate receptor types results in a specificity toward a chosen receptor composition, thus demonstrating a general route toward targeting cells without particularly dominant markers.

We have assumed a generic case where background (untargeted) cell populations contain all possible receptor compositions. However, the selectivity can be increased further if only a few distinct cell populations are present and their receptor compositions are known in advance. In this case the optimal targeting strategy is obtained by maximizing the free-energy difference between discreet populations rather than the free-energy curvature. We also note that, although in this paper we focus on the targeting of cells, our model can also be used to understand how imprinted polymers can be used to sort cells (12, 13).

Materials and Methods

Endocytosis Simulations. We perform Monte Carlo simulations with a coarse-grained membrane model (14) and a patchy hard-sphere model (15) for the nanoparticle. The nanoparticle has two different types of circular patches modeling coverage with two different ligand types. The membrane is composed of individual beads that can be either inert (representing normal lipids) or "receptor" beads that bind to the cognate patches on the particle, but are otherwise identical to the inert beads. The receptor beads can interact with the patches via a square-well attraction with width σ equal to the diameter of individual beads σ, where ϵ denotes the well depth. The particle wrapping is calculated as the number of membrane beads within a distance σ of the particle surface N_w, normalized by the fully wrapped triangular lattice, $w = N_w \frac{\sqrt{3}}{2\pi(R+\sigma)^2}$, with $R = 4\sigma$ the particle radius.

The simulations are performed using standard Monte Carlo translational moves in the *NpT* ensemble and no applied external pressure (to be precise, our membrane system is metastable at zero applied external pressure, and the thermodynamically stable configuration is an infinitely large box; however, on a simulation timescale, a flat membrane is stable). The box size is $40\sigma \cdot 40\sigma$ with periodic boundary conditions in lateral directions. The box size in the vertical z direction is sufficiently large to ensure that none of the particles ever interacts with the hard ceiling or the floor. The simulations started with the particle center of mass at height $R + \sigma$ above the membrane and were run for $6 \cdot 10^6$ cycles, where in each cycle on average one translational/rotational move per every bead and particle is attempted.

Multivalent Particle Adsorption. We performed grand canonical Monte Carlo simulations where the chemical potential of the guest particles in solution is fixed to a value that results in a desired guest density in solution. Guest particles are represented as hard spheres with radius $R = 3r_b$ and attached polymeric ligand arms that are modeled as a series of soft blobs of size r_b (16). Receptors are represented as points on the hard surface and can bind to ligands with a valence-limited harmonic bond and the interaction matrix ϵ determines the individual binding/unbinding probabilities. Standard Monte Carlo moves are used to displace and add/delete guests into the system, and Rosenbluth sampling is used to change polymeric ligand conformations. The model and technique are an extension of ref. 5 to multiple ligand/receptor types.

Free energies are calculated using the Wang–Landau sampling technique (17). First, we bias the sampling in the number of formed ligand–receptor bonds to obtain the absolute value of the bound guest free energy relative to a common reference point: a single unbound guest particle within interaction range h_0 of the surface ($h_0 = 3r_b$ for single-blob ligands and can be well approximated as the average height of a guest with a single formed bond). We then bias the simulation in the receptor composition to obtain the curvature of the free energy. The selectivity $\mathcal{S}$ is calculated by fitting a quadratic function to the free-energy profile and normalizing by the absolute value as in Eq. **4**. Langmuir isotherm (Fig. 4) zero-bond free energy is approximated as the translational entropy of a guest within a lattice site of size A and height h_0: $\Delta F_0 = -k_B T \log(A h_0 \rho_0 N_A)$.

ACKNOWLEDGMENTS. We thank Bortolo Mognetti and Stefano Angioletti-Uberti for in-depth discussions on multivalency and Anđela Šarič for help with endocytosis simulations. This work was supported by the European Union through European Training Network NANOTRANS Grant 674979 and by the Herchel Smith fund.

1. Mura S, Nicolas J, Couvreur P (2013) Stimuli-responsive nanocarriers for drug delivery. *Nat Mater* 12:991–1003.
2. Wilhelm S, et al.(2016) Analysis of nanoparticle delivery to tumours. *Nat Rev Mater* 1:14–26.
3. Caplan MR, Rosca EV (2005) Targeting drugs to combinations of receptors: A modeling analysis of potential specificity. *Ann Biomed Eng* 33:1113–1124.
4. Robinson MK, et al. (2008) Targeting ErbB2 and ErbB3 with a bispecific single-chain Fv enhances targeting selectivity and induces a therapeutic effect in vitro. *Br J Cancer* 99:1415–1425.
5. Martinez-Veracoechea FJ, Frenkel D (2011) Designing super selectivity in multivalent nano-particle binding. *Proc Natl Acad Sci USA* 108:10963–10968.
6. Dubacheva GV, et al. (2014) Superselective targeting using multivalent polymers. *J Am Chem Soc* 136:1722–1725.
7. Dubacheva GV, Curk T, Auzély-Velty R, Frenkel D, Richter RP (2015) Designing multivalent probes for tunable superselective targeting. *Proc Natl Acad Sci USA* 112:5579–5584.
8. Carlson CB, Mowery P, Owen RM, Dykhuizen EC, Kiessling LL (2007) Selective tumor cell targeting using low-affinity, multivalent interactions. *ACS Chem Biol* 2:119–127.
9. Kiessling LL, Grim JC (2013) Glycopolymer probes of signal transduction. *Chem Soc Rev* 42:4476–4491.
10. Bell GI, Dembo M, Bongrand P (1984) Cell adhesion. Competition between nonspecific repulsion and specific bonding. *Biophys J* 45:1051–1064.
11. Xu H, Shaw DE (2016) A simple model of multivalent adhesion and its application to influenza infection. *Biophys J* 110:218–233.
12. Ren K, Zare RN (2012) Chemical recognition in cell-imprinted polymers. *ACS Nano* 6:4314–4318.
13. Ren K, Banaei N, Zare RN (2013) Sorting inactivated cells using cell-imprinted polymer thin films. *ACS Nano* 7:6031–6036.
14. Yuan H, Huang C, Li J, Lykotrafitis G, Zhang S (2010) One-particle-thick, solvent-free, coarse-grained model for biological and biomimetic fluid membranes. *Phys Rev E* 82:011905.
15. Kern N, Frenkel F (2003) Fluid-fluid coexistence in colloidal systems with short-ranged strongly directional attraction. *J Chem Phys* 118:9882–9889.
16. Pierleoni C, Capone B, Hansen J-P (2007) A soft effective segment representation of semidilute polymer solutions. *J Chem Phys* 127:171102.
17. Wang F, Landau DP (2001) Efficient, multiple-range random walk algorithm to calculate the density of states. *Phys Rev Lett* 86:2050–2053.

Optimal multivalent targeting of membranes with many distinct receptors

Curk, Tine; Dobnikar, Jure; Frenkel, Daan

01 Santiago Rodriguez Page 1
5/4/2024 12:53

02 Santiago Rodriguez Page 1
5/4/2024 9:04

03 Santiago Rodriguez Page 1
5/4/2024 9:04

04 Santiago Rodriguez Page 1
5/4/2024 9:06

05 Santiago Rodriguez Page 1
5/4/2024 12:57

06 Santiago Rodriguez Page 1
5/4/2024 12:57

07 Santiago Rodriguez Page 1
5/4/2024 12:57

08 Santiago Rodriguez Page 1
5/4/2024 12:58

09 Santiago Rodriguez Page 1
5/4/2024 13:03

10 Santiago Rodriguez Page 1

5/4/2024 13:03

11 Santiago Rodriguez Page 1

5/4/2024 12:52

12 Santiago Rodriguez Page 1

5/4/2024 12:53

13 Santiago Rodriguez Page 1

5/4/2024 12:53

14 Santiago Rodriguez Page 2

5/4/2024 13:23

15 Santiago Rodriguez Page 2

5/4/2024 13:23

16 Santiago Rodriguez Page 2

5/4/2024 13:23

17 Santiago Rodriguez Page 2

5/4/2024 13:24

18 Santiago Rodriguez Page 2

5/4/2024 14:41

Assume that there are 2 types of ligands and cognate receptors. Sketch all the possible interactions between ligands and receptors when

a) K is diagonal
b) K is non-diagonal

19 Santiago Rodriguez Page 2

5/4/2024 13:28

20 Santiago Rodriguez Page 2

5/4/2024 13:03

21 Santiago Rodriguez Page 2

5/4/2024 13:28

22 Santiago Rodriguez Page 2

5/4/2024 13:29

23 Santiago Rodriguez Page 2

5/4/2024 13:31

24 Santiago Rodriguez Page 2

5/4/2024 13:04

25 Santiago Rodriguez Page 2

5/4/2024 13:31

26 Santiago Rodriguez Page 2

5/4/2024 13:33

27 Santiago Rodriguez Page 2

5/4/2024 13:06

28 Santiago Rodriguez Page 2

5/4/2024 13:06

29 Santiago Rodriguez Page 2

5/4/2024 13:10

30 Santiago Rodriguez Page 2

5/4/2024 13:10

31 Santiago Rodriguez Page 2

5/4/2024 13:10

32 Santiago Rodriguez Page 2

5/4/2024 13:14

33 Santiago Rodriguez Page 2

5/4/2024 13:15

34 Santiago Rodriguez Page 2

5/4/2024 13:19

35 Santiago Rodriguez Page 2

5/4/2024 13:20

36 Santiago Rodriguez Page 2

5/4/2024 13:20

37 Santiago Rodriguez Page 2

5/4/2024 13:20

38 Santiago Rodriguez Page 2

5/4/2024 13:20

39 Santiago Rodriguez Page 2

5/4/2024 13:20

40 Santiago Rodriguez Page 2

5/4/2024 13:23

41 Santiago Rodriguez Page 2

5/4/2024 13:23

42 Santiago Rodriguez Page 2

5/4/2024 13:23

43 Santiago Rodriguez Page 2

5/4/2024 13:23

44 Santiago Rodriguez Page 2

5/4/2024 13:23

45 Santiago Rodriguez Page 3

5/4/2024 13:56

46 Santiago Rodriguez Page 3

5/4/2024 14:02

47 Santiago Rodriguez Page 3

5/4/2024 14:02

48 Santiago Rodriguez Page 3

5/4/2024 14:02

49 Santiago Rodriguez Page 3

5/4/2024 14:06

50 Santiago Rodriguez Page 3

5/4/2024 14:19

51 Santiago Rodriguez Page 3

5/4/2024 14:19

52 Santiago Rodriguez Page 3

5/4/2024 14:08

53 Santiago Rodriguez Page 3

5/4/2024 13:45

54 Santiago Rodriguez Page 3

5/4/2024 13:45

55 Santiago Rodriguez Page 3

5/4/2024 13:46

56 Santiago Rodriguez Page 3

5/4/2024 13:46

57 Santiago Rodriguez Page 3

5/4/2024 13:46

58 Santiago Rodriguez Page 3

5/4/2024 13:46

59 Santiago Rodriguez Page 3

5/4/2024 14:11

60 Santiago Rodriguez Page 3

5/4/2024 14:11

61 Santiago Rodriguez Page 3

5/4/2024 14:11

62 Santiago Rodriguez Page 3

5/4/2024 13:46

63 Santiago Rodriguez Page 3

5/4/2024 13:46

64 Santiago Rodriguez Page 3

5/4/2024 13:46

65 Santiago Rodriguez Page 3

5/4/2024 14:11

66 Santiago Rodriguez Page 3

5/4/2024 13:46

67 Santiago Rodriguez Page 3

5/4/2024 13:56

68 Santiago Rodriguez Page 3

5/4/2024 13:55

69 Santiago Rodriguez Page 3

5/4/2024 14:12

70 Santiago Rodriguez Page 4

5/4/2024 14:20

71 Santiago Rodriguez Page 4

5/4/2024 14:20

72 Santiago Rodriguez Page 4

5/4/2024 14:21

73 Santiago Rodriguez Page 4

5/4/2024 14:45

74 Santiago Rodriguez Page 4

5/4/2024 14:13

75 Santiago Rodriguez Page 4

5/4/2024 14:13

76 Santiago Rodriguez Page 4

5/4/2024 14:45

77 Santiago Rodriguez Page 4

5/4/2024 14:45

78 Santiago Rodriguez Page 4

5/4/2024 14:45

79 Santiago Rodriguez Page 4

5/4/2024 14:14

80 Santiago Rodriguez Page 4

5/4/2024 14:14

81 Santiago Rodriguez Page 4

5/4/2024 14:25

82 Santiago Rodriguez Page 4

5/4/2024 14:25

83 Santiago Rodriguez Page 4

5/4/2024 14:17

84 Santiago Rodriguez Page 5

5/4/2024 9:13

85 Santiago Rodriguez Page 5

5/4/2024 9:13

86 Santiago Rodriguez Page 5

5/4/2024 9:14

87 Santiago Rodriguez Page 5

5/4/2024 9:14

88 Santiago Rodriguez Page 5

5/4/2024 14:56

89 Santiago Rodriguez Page 5

5/4/2024 9:14

90 Santiago Rodriguez Page 5

5/4/2024 14:57

91 Santiago Rodriguez Page 5

5/4/2024 9:25

92 Santiago Rodriguez Page 5

5/4/2024 9:23

93 Santiago Rodriguez Page 5

5/4/2024 9:23

94 Santiago Rodriguez Page 5

5/4/2024 14:58

95 Santiago Rodriguez Page 5

5/4/2024 9:25

96 Santiago Rodriguez Page 5

5/4/2024 9:25

97 Santiago Rodriguez Page 5

5/4/2024 14:59

98 Santiago Rodriguez Page 5

5/4/2024 14:59

99 Santiago Rodriguez Page 5

5/4/2024 14:59

100 Santiago Rodriguez Page 5

5/4/2024 14:59

101 Santiago Rodriguez Page 5

5/4/2024 14:59

102 Santiago Rodriguez Page 5

5/4/2024 14:59

103 Santiago Rodriguez Page 5

5/4/2024 14:59

104 Santiago Rodriguez Page 5

5/4/2024 15:01

105 Santiago Rodriguez Page 5

5/4/2024 15:01

106 Santiago Rodriguez Page 5

5/4/2024 15:01